

## Article

# The Incorporation of Ladle Furnace Slag in Fire Insulating Gypsum-Based Materials

Begoña Peceño <sup>1</sup>, Eva M. Pérez-Soriano <sup>2</sup>, Yolanda Luna-Galiano <sup>3</sup> and Carlos Leiva <sup>3,\*</sup>

<sup>1</sup> Escuela de Prevención de Riesgos y Medioambiente, Facultad de Ciencias del Mar, Universidad Católica del Norte, Larrondo 1281, Coquimbo 1781421, Chile; begopc@ucl.cl

<sup>2</sup> Department of Materials Science and Engineering and Transport, Escuela Politécnica Superior, Universidad de Sevilla, 41011 Seville, Spain; evamps@us.es

<sup>3</sup> Department of Chemical and Environmental Engineering, Escuela Superior de Ingenieros, Universidad de Sevilla, 41092 Seville, Spain; yluna@us.es

\* Correspondence: cleiva@us.es; Tel.: +34-954487270

**Abstract:** Ladle slag, a byproduct of steel manufacturing, exhibits inherent reactivity and undergoes hydration when exposed to water. Nevertheless, these reaction byproducts often remain metastable, leading to microstructural alterations when incorporated into cementitious materials, thereby limiting the recycling potential of ladle slag. This study explores the fire insulating capacity and the physical, mechanical, and leaching characteristics of gypsum-based materials with substantial quantities of ladle slag in instead of gypsum. The mechanical strength of the specimens declines as the ladle slag content increases. Nevertheless, the percentage decrease in compressive strength at various temperatures (300 °C, 500 °C, and 700 °C) is less pronounced when higher amounts of ladle slag are used. Fire-resistant properties, assessed using the EN 1363-1 standards, diminish with increasing slag proportions; although the inclusion of ladle slag introduces certain endothermic processes that positively affect the fire insulating capacity, resulting in a 20% reduction when 60%wt of slag is employed. Notably, no gas emissions were observed during the fire test, indicating the absence of environmental hazards. In conclusion, ladle slag does not pose a leaching threat to the environment, making it a viable and sustainable alternative to gypsum in gypsum-based materials.

**Keywords:** ladle slag; fire insulating capacity; compressive strength; leaching



**Citation:** Peceño, B.; Pérez-Soriano, E.M.; Luna-Galiano, Y.; Leiva, C. The Incorporation of Ladle Furnace Slag in Fire Insulating Gypsum-Based Materials. *Fire* **2023**, *6*, 416. <https://doi.org/10.3390/fire6110416>

Academic Editors: Yan Ding, Keqing Zhou and Kaili Gong

Received: 5 October 2023

Revised: 21 October 2023

Accepted: 25 October 2023

Published: 27 October 2023



**Copyright:** © 2023 by the authors. Licensee MDPI, Basel, Switzerland. This article is an open access article distributed under the terms and conditions of the Creative Commons Attribution (CC BY) license (<https://creativecommons.org/licenses/by/4.0/>).

## 1. Introduction

The production of steel using the electric arc furnace method comprises two distinct phases. In the initial phase, referred to as primary metallurgy or the melting process, scrap materials are melted alongside fluxes in the electric furnace, resulting in molten metal accompanied by liquid slags known as Electric Arc Furnace Slags or black slags, which form on the surface. The subsequent phase, known as secondary metallurgy or the refining process, involves transferring the molten bath to the Ladle Furnace for desulfurization, degassing, and adjustment of its chemical composition. The slag generated during this second phase is called white or ladle slag. The manufacture of each ton of steel via this method involves the generation of roughly 20 to 30 kg of ladle slag and 120 to 180 kg of black slag. In Spain, steel production reached 13.6 million tons in 2019 [1], resulting in the generation of approximately 0.19 to 0.29 million tons of ladle slag. Globally, in 2023, projections indicate that the production of ladle slag will exceed 20 million tons [2].

Currently, there are few viable alternatives for the utilization of white slag, leading to its predominant disposal in landfills. This is primarily due to issues related to its volume instability, stemming from the crystallization of free-CaO and free-MgO during the cooling process. However, there are interesting applications for white slag in the future, such as in clinker manufacture and as a partial substitute for aggregates and/or cement in mortars [3,4] and concretes. Additionally, white slag can find use in soil and firm

stabilization [5], asphalt pavement construction [6,7], the production of alkali-activated cements [8,9], brick manufacturing [10], waterproofing beds in hydraulic or fluvial works [11], soil acidity correction in agriculture [12], the fixation of ions in water purification processes in environmental engineering [13], and the development of fishing blocks in aquaculture [13].

Given the inherent lack of fire resistance in various construction materials, it is essential to explore fire protection methods [14]. These measures typically fall into two categories: active, which involve automated detection and suppression systems, and passive, which focus on slowing the spread of fire. In this second category, the primary goal is to maintain a component's temperature below its critical threshold to prevent structural collapse [15]. Some studies have analyzed the use of different waste materials in the development of passive fire protection materials. These materials include coal and biomass fly/bottom ashes [16–19], polyamide powder waste [20], mollusk shells [21], titanium dioxide waste [22], granulated blast furnace slag [23], and polyurethane foam waste [24].

As previously mentioned, ladle slag contains significant percentages of certain elements [25], and as a result it might be used as an alternative component of fire insulating materials. Utilizing ladle slag in this context offers sustainability benefits by reducing our reliance on natural resources without any leaching problems, while providing adequate fire resistance and stable strength development and reducing gypsum consumption.

## 2. Materials and Methods

### 2.1. Materials and Tested Mixtures

The ladle slag used in this study is from a hot steel foundry and rolling plant located in the southern region of Spain. As depicted in Figure 1, the ladle slag exhibits a distinctive white coloration. These slags come from the secondary phase of refining molten steel. Initially, white slag is stored in designated slag bins within the manufacturing facility. Subsequently, the white slag undergoes a conditioning process, encompassing physical cooling treatment, metal separation, and size reduction. In Section 3.1, a comprehensive analysis of the ladle slag's chemical and mineralogical characteristics is provided. For the binding agent, gypsum, in accordance with EN 13279-1:2009 [26], was utilized.



**Figure 1.** Ladle slag.

Table 1 illustrates the various compositions formulated in this study, wherein varying proportions (ranging from 40% to 80% by weight) of gypsum were substituted with ladle slag. The quantity of incorporated water was adjusted to ensure consistent paste fluidity. As observed in Table 1, when the gypsum content was decreased, it was necessary to decrease the water; because the water was not used in the hydration reaction ( $\text{CaSO}_4 + 2\text{H}_2\text{O} \rightarrow \text{CaSO}_4 \cdot 2\text{H}_2\text{O}$ ) of the gypsum, it produced a supernatant on top of the samples in the molds and decreased the size of the samples after setting. All components were thoroughly blended using a laboratory kneader. Initially, gypsum and ladle slag were

introduced into the kneader and mixed for a duration of 5 min. Subsequently, water was incorporated to the solid blend, and everything was mixed until a homogenous paste was formed. The molds for the various tests were then filled. The samples were removed from the molds after 24 h at room temperature. These samples were then allowed to cure for a further 27 days in a chamber with a temperature of 25 °C and a humidity level of 65%.

**Table 1.** Mixing ratios of the various materials.

Sample	Gypsum [%wt]	Ladle Slag [%wt]	Water/Solid Ratio
Gypsum	100	0	0.45
ESC 40	60	40	0.42
ESC 50	50	50	0.41
ESC 60	40	60	0.40
ESC 80	20	80	0.39

## 2.2. Chemical, Mineralogical, and Physical Properties

Since the ladle slag was received in dust form ( $D_{50} = 36 \mu\text{m}$ ), no previous treatment (milling or sieving) was performed. The major and trace components were identified via X-ray fluorescence spectroscopy analysis (Bruker AXS GmbH, Karlsruhe, Germany) at the Research, Technology, and Innovation Center at the University of Seville (CITIUS). The analysis of slag required that the sample be placed into a plastic sample cup with a plastic support film. This insured a flat surface for the X-ray analyzer and the sample to be supported over the X-ray beam. This requirement can be met by using 15 g of ladle slag to insure definite thickness for all of elements of interest.

The XRD analysis of ladle slag was carried out using a D8 Advance A25 instrument (BRUKER) (40 kV and 30 mA). The DIFFRAC-EVA version 7 software (BRUKER) was used for phase identification. The software works with a reference database ICDD PDF4.2022 version of JCPDS. Phase identification and accurate quantitative phase analysis (amorphous and crystalline contents) were based on the reference intensity ratio (RIR) method.

The sample density was determined by calculating the average of six sample weights, with a precision of  $\pm 0.1$  g, and volume measurements were conducted following the 1097-7 standard method [27]. To assess the water absorption capacity (A), the guidelines outlined in EN 12859 [28] were followed, using three cylindrical samples.

## 2.3. Mechanical Properties

Following the manufacture of the samples, experimental tests to determine their mechanical characteristics were conducted. To ensure representative values, each test involved three specimens. Surface hardness established was as defined in EN 12859 [28], using a durometer. For each sample, six measurements were taken on various faces, which are given in Shore C units.

Compressive strength was assessed following ASTM-E-761-81 [29] at 28 days after manufacturing. Additionally, the compressive strength evolution after 3 h of exposure at high temperatures (300, 500, and 700 °C) was studied. The resistance index ( $RI_T$ ) was obtained according to the following formula:

$$RI_T = \frac{100 \cdot R_T}{R_{25}} \quad (1)$$

where  $R_{25}$  represents the compressive strength after 28 days, and  $R_T$  represents the compressive strength after exposure at  $T$  °C. Three samples were evaluated for each dosage and temperature.

## 2.4. Fire Insulating Capacity

The time necessary to reach a temperature of 550 °C ( $t_{550}$ ) in the center of the sample is referred as the fire insulating capacity. As illustrated in Figure 1, cylindrical samples were

subjected to controlled heating as defined in EN 1363-1 [30] and consistent with previous research [22,23]. To ensure uniform heat distribution, ceramic fibers were employed to insulate both the bottom and top surfaces of the cylinder. Consequently, the samples encountered radial heat flow, which is symmetric. The relationship between fire temperature ( $T$ ) and exposure time ( $t$ ) can be expressed as  $T = 20 + 345 \cdot \log(t + 1)$ . For this test, as it can be seen in Figure 2, larger cylinder molds were required, with dimensions of 4.2 cm in diameter and 20 cm in height, including a 10 cm wire placed centrally. This test was conducted after a curing period of 28 days. This wire served a dual purpose, facilitating the placement of a thermocouple, which measures the interior temperature of the cylinder upon entering the oven, and acting as a structural support. The critical parameter in this test is the time taken for the center of the cylinder to reach 550 °C ( $t_{550}$ ), which signifies the onset of failure of the protective metal structure intended to shield the material from the fire.

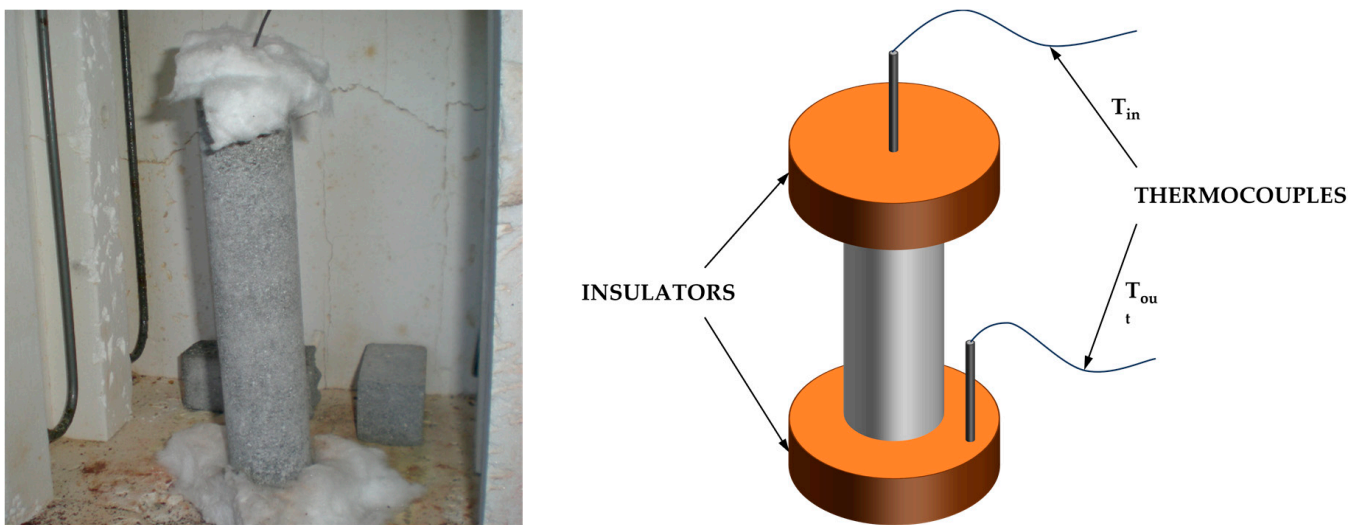


**Figure 2.** Real image (left) and sketch diagram (right) of the fire insulating capacity test.

### 2.5. Differential Scanning Calorimetry (DSC) Test

A DSC analysis was conducted to assess the amount of heat energy absorbed by the ladle slag in the heating process. Ladle slag was carefully deposited in aluminum containers and heated at a rate of 2 °C per minute, ranging from 25 to 500 °C. Nitrogen gas was employed as the purging gas throughout the test, following established procedures [18].

### 2.6. Leaching Test

In Europe, there is currently no standardized approach to classifying slag, leading to a divergence in practices among countries. Some nations view slag as a valuable by-product and have specific regulations in place, while others continue to regard steel-making slag as mere trash. Of particular concern are the potential pollutants associated with slags, including heavy metals (for example Mn, Cu, Cr, Zn, As, Pb, Cd, Hg, Ni) [31]. These metals could be involved in a leaching process when slags are incorporated into construction materials. To meet the criteria for classification as building materials, the products developed in this study must exhibit low toxicity levels. Leaching tests were conducted in accordance with EN 12457-4 [32] to characterize both ladle slag and gypsum, facilitating a comparative analysis of their leaching behavior.

## 3. Results and Discussion

### 3.1. Ladle Slag Characterization

Table 2 presents the major and minor components of ladle slag established via X-ray fluorescence. The chemical compositions of ladle slag can exhibit variations due to the

furnace type, the furnace load's composition, the steel grades being produced, and the operational methods of each furnace [33]. Ladle slag typically has a high CaO content, though it falls towards the lower end of the typical range (45–62% by weight). The precise CaO content is contingent upon the quantity of lime added during the production process. In addition, SiO<sub>2</sub> is also present, generally falling within the range of 17.4–19.3%. MgO typically exhibits components within a range of 4.5–17.2% by weight; these values are primarily influenced by the use of dolomite and interactions between the slag and the furnace lining, which typically contains a substantial amount of MgO. Al<sub>2</sub>O<sub>3</sub> is typically found in a range between 3.2–10.4% by weight. During the refining stage to which liquid steel is subjected, silica or alumina is added, which will be reflected in the chemical composition of the slag. As evident in Table 2, SiO<sub>2</sub> was added during the refining phase in this particular case. Ladle slag may contain trace amounts of potential pollutants (heavy metals such as Cr, Mn, Zn, Pb, and Ba), which could lead to environmental concerns, particularly in terms of leaching, when the slag is utilized in construction materials that come into contact with water.

**Table 2.** Major and minor components of ladle slag.

Major Components	[%wt]	Minor Components	[ppm]
SiO <sub>2</sub>	15.03	S	133.56
Fe <sub>2</sub> O <sub>3</sub>	2.33	Cr	28.25
FeO	1.08	P	4.31
Al <sub>2</sub> O <sub>3</sub>	6.23	Zn	293
CaO	45.20	Ti	41.74
MgO	13.35	Sr	3.05
MnO	1.48	Cu	180
Loss on ignition	14.16	Cl	22.61
Specific gravity	2.88	Ba	292
	data	Pb	72

The specific gravity of ladle slag, as determined by EN 1097-7 [34], is notably 30% lower than that of gypsum (4.06 g/cm<sup>3</sup>), as shown in Table 2. The mineralogical characterization, depicted in Figure 3 through X-Ray diffraction, reveals the predominant presence of calcium silicates (larnite, gehlenite, calcium silicate sulfate, calcium silicate), calcium–magnesium (merwinite), and ferric (hedenbergite) phases, accompanied by quartz, calcite, and brucite. An estimate of the percentage of amorphous and crystalline material in the sample, obtained by comparing the area under the curve corresponding to the material with diffraction lines and the area encompassed by the rest of the diffractogram, indicates that the sample comprises 67% crystalline phase and 33% amorphous phase.

Additionally, the particle size distributions of both gypsum and white slag were assessed using a Saturn DigiSizer II 5205 in an inert medium, with isopropanol for ladle slag and water for gypsum. Ladle slag presented a particle size interval lower than 400 µm. Ladle slag presented a D<sub>50</sub> of 36 µm, and the gypsum 30 µm.

Figure 4 reveals multiple endothermic peaks during the heating of the slag. At 50 °C, there is a peak attributed to the evaporation of moisture. Around 120 °C, another peak corresponds to the evaporation of chemically bound water within sulfur compounds. A subtle peak at approximately 170 °C is related to the dehydration of metastable calcium aluminate hydrate phases [35]. The prominent endothermic peak observed at 300 °C is linked to the dehydration of stable calcium aluminate hydrates [36]. The endothermic peak at approximately 450 °C is indicative of portlandite decomposition.

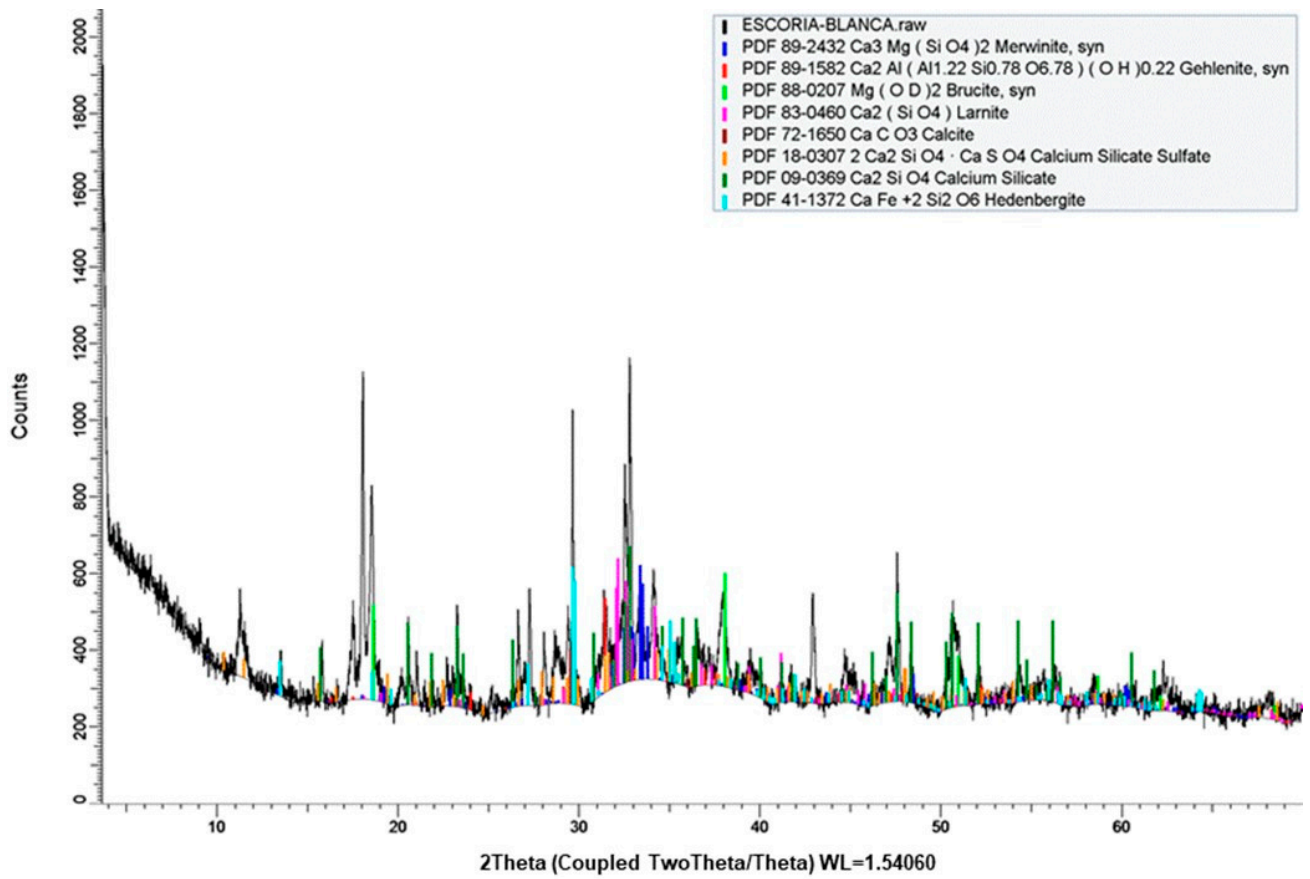


Figure 3. X-Ray diffraction of ladle slag.

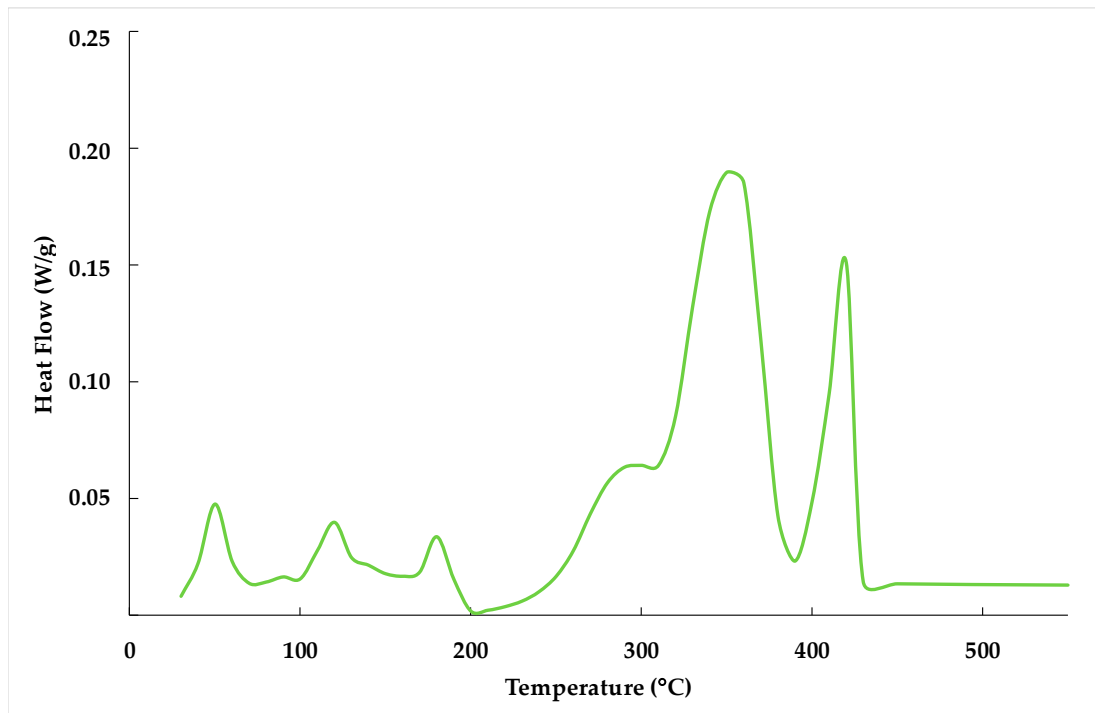


Figure 4. Differential scanning calorimetry analysis of ladle slag.

### 3.2. Physical Characterization of the Mixtures

Figure 5 depicts the density variations among the different mixtures. Notably, an increase in ladle slag content results in a decrease in density. This can primarily be attributed to ladle slag's lower specific density (as indicated in Table 2) compared to gypsum. Additionally, the slightly larger particle size of the slag also produces a decrease in density. According to EN 12859, gypsum-based materials can be classified into three categories based on their density: high (between 1100 and 1500 kg/m<sup>3</sup>), medium (between 800 and 1100 kg/m<sup>3</sup>), and low (between 600 and 800 kg/m<sup>3</sup>). All the compositions in this study fall under the high-density classification. Figure 6 illustrates the water absorption characteristics of the various mixtures. Water absorption capacity exhibits an inverse relationship with density; the lower the density, the greater the porosity, and therefore the greater the volume of voids available for water absorption.

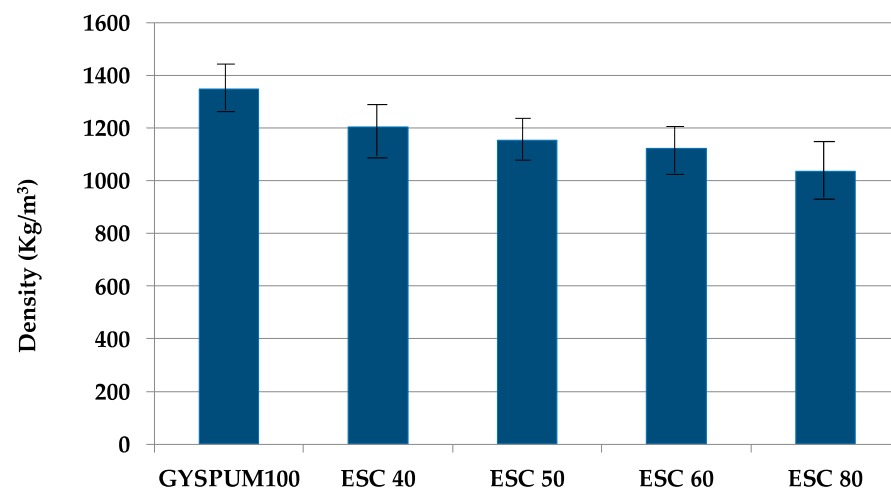


Figure 5. Density variation among the different mixtures.

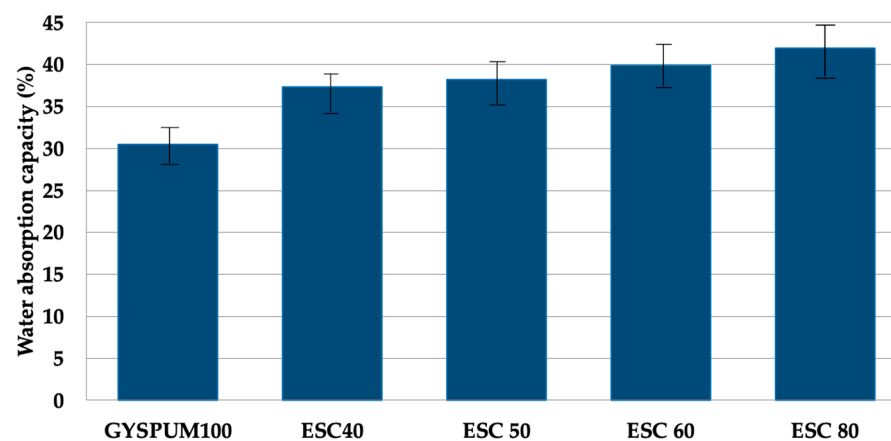
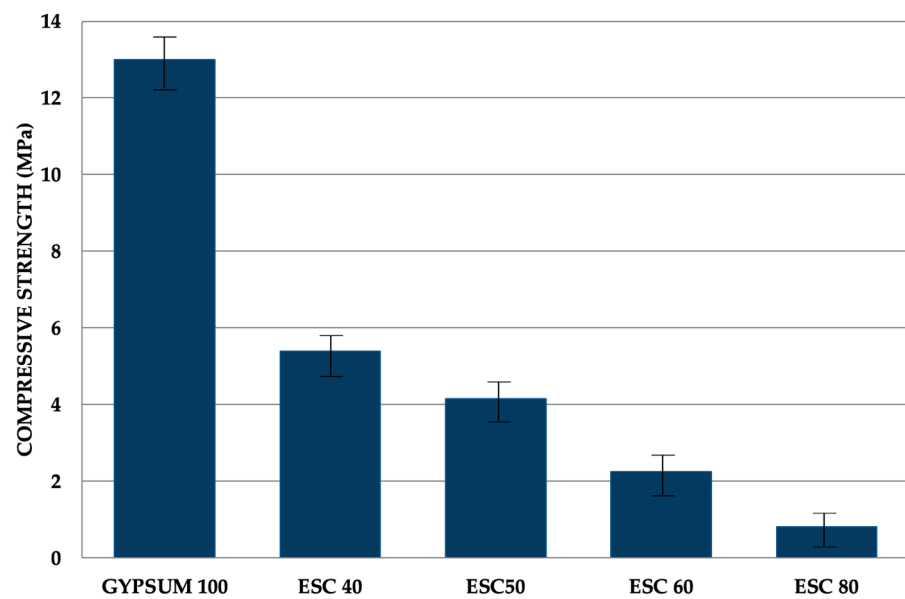


Figure 6. Water absorption of the different mixtures.

### 3.3. Mechanical Characterization of the Mixtures

Figure 7 shows the compressive strength values of the mixtures. It is noticeable that increasing the quantity of slag reduces compressive strength. These findings demonstrate a clear inverse relationship with porosity. As per EN 13279-1 [26], the standard specifies that the compressive strength of gypsum-based materials should be equal to or exceed 2 MPa, a requirement that all samples, except ESC 80, meet.



**Figure 7.** Compressive strength of different mixtures at ambient temperature.

Figure 8 shows the evolution of the  $RI_T$  of the different compositions at ambient temperature, 300 °C, 500 °C, and 700 °C. The compressive strength of gypsum experiences a significant decrease at 300 °C due to an endothermic reaction, the dehydration of gypsum ( $\text{CaSO}_4 \cdot 2\text{H}_2\text{O} \rightarrow \text{CaSO}_4 + 2\text{H}_2\text{O}$ ), which occurs within the temperature range of 120 to 150 °C [37]. At higher temperatures, the reduction in the  $RI_T$  is much less pronounced because gypsum does not undergo any reactions leading to mass losses. At 300 °C, the decrease in  $RI_T$  is less pronounced when the ladle slag percentage is higher, primarily due to the lower mass loss exhibited by the slag. At 500 °C, a noticeable reduction in  $RI_T$  is observed in mixtures containing predominantly ladle slag, due to the dehydration of metastable calcium aluminate hydrates (Figure 4). At 700 °C, the compressive strength of samples with a substantial amount of gypsum decreases because the gypsum used in the mix contains additional calcium carbonate in its dosage. The decrease in the compressive strength of samples with a relevant amount of ladle slag is only slightly lower than at 500 °C. This reduction is primarily attributed to the decomposition of portlandite at 450 °C and minor weight loss peaks associated with the decomposition of carbonates, occurring between 680 °C and 800 °C.

Macroscopic observations of the samples, depicted in Figure 9, reveal that at 300 °C there are no visible cracks on the specimen surfaces. However, at 700 °C, the degree of deterioration has increased compared to gypsum-based samples. It is evident that spalling phenomena have occurred at 700 °C. Significantly, a distinct pattern becomes evident: as the quantity of slag increases and the temperature rises, the compressive strength values of the mixtures decrease.

Figure 10 shows the surface hardness values measured from the various samples after 28 days of setting. The higher the proportion of white slag, the lower the hardness value. The EN 12859 standard [28] dictates the specifications for superficial hardness that materials must meet according to their density classification, which categorizes them as high (>80 Shore C), medium (>55 Shore C), or low density (>40 Shore C). Of the different compositions, only those with less than 50% ladle slag content exhibit values surpassing the threshold for high-density materials. Surface hardness is a property that exhibits a direct inverse relationship with porosity. A higher porosity produces a lower hardness, as in study [19].

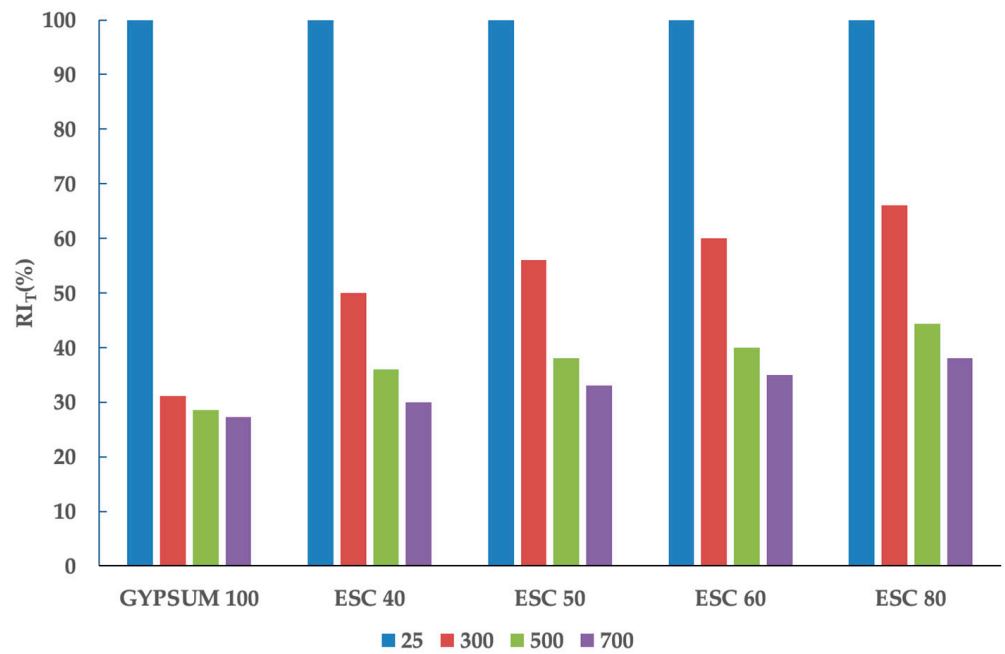


Figure 8.  $RI_T$  of the different mixtures.

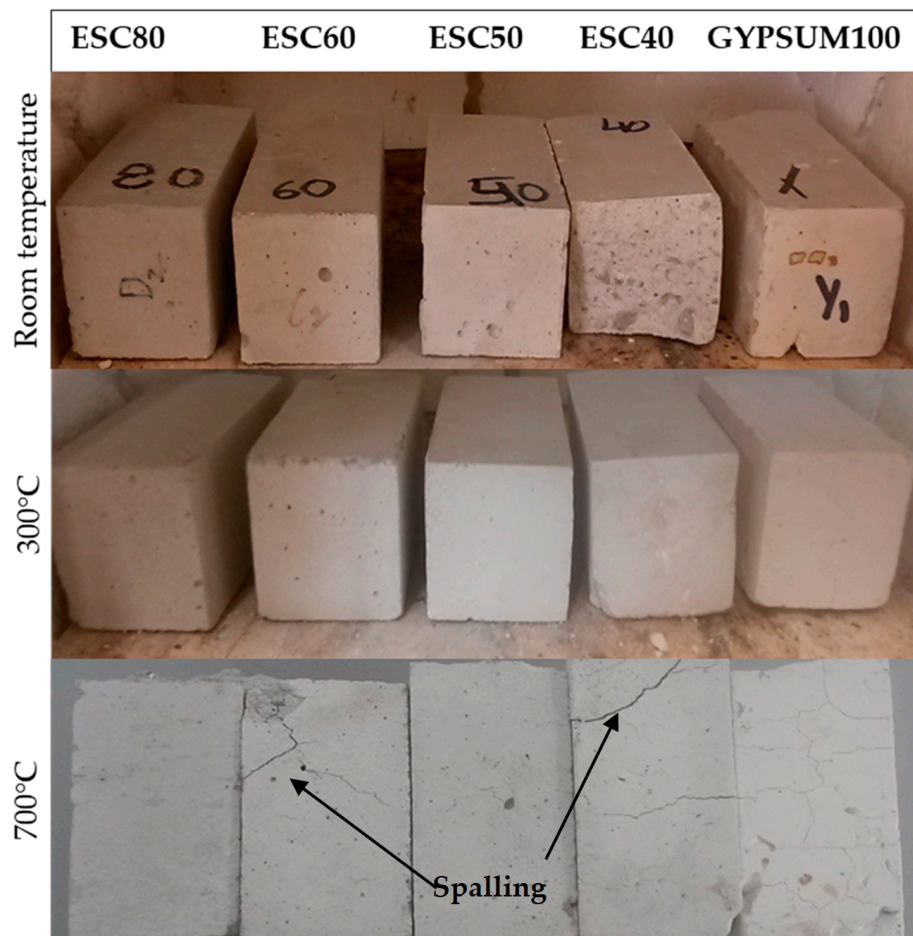


Figure 9. Macroscopic examination of various mixtures at different temperatures.

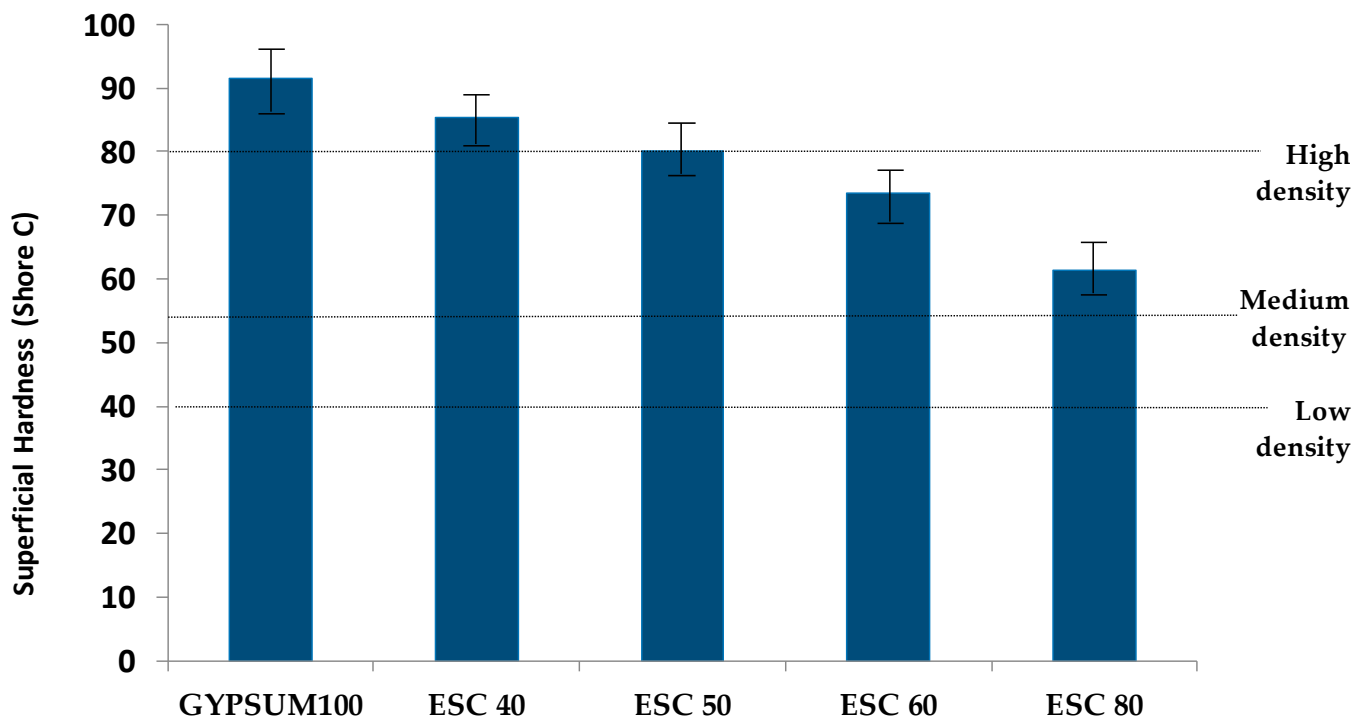


Figure 10. Superficial hardness of the different mixtures.

### 3.4. Fire Insulating Capacity

Figure 11 illustrates the fire insulating capability of the various mixtures. As the water-solid is increased when the dosage of the ladle slag is, this produces a high porosity, increasing the humidity retained in the pores; this water is evaporated at temperatures around 50 °C, decreasing the slope of the curves before the evaporation plateau. The chemically bound water content in gypsum-based materials plays a crucial role in enhancing fire-resistant behavior, as it prolongs the time required to reach 100 °C. Interestingly, a higher ladle slag content results in a shorter time needed to reach 100 °C. At 100 °C, there is a sustained period during which the temperature remains constant, attributable to the endothermic dehydration reaction of gypsum ( $\text{CaSO}_4 \cdot 2\text{H}_2\text{O} \rightarrow \text{CaSO}_4 + 2\text{H}_2\text{O}$ ). This reaction absorbs the energy transmitted by the fire, thus keeping the temperature constant at the core of the cylinder. While the inclusion of ladle slag introduces calcium aluminate hydrates, which also undergo endothermic decomposition, the energy absorbed by these hydrates is less than that absorbed during gypsum dehydration. Therefore, the duration of the evaporation plateau decreases with increasing ladle slag content. Beyond the evaporation plateau, the introduction of ladle slag results in the emergence of new, smaller evaporation plateaus (e.g., at 170 °C for the dehydration of metastable calcium aluminate hydrates, at 300 °C for the dehydration of stable calcium aluminate hydrates, and at 450 °C for the decomposition of portlandite). For this reason, the differences in  $t_{550}$  between Gypsum100 and samples with slag additions are smaller than the disparities in the duration of the evaporation plateau. For instance, in the case of ESC60, the length of the evaporation plateau is 50% shorter than that of Gypsum100, but the  $t_{550}$  is only reduced by 18%.

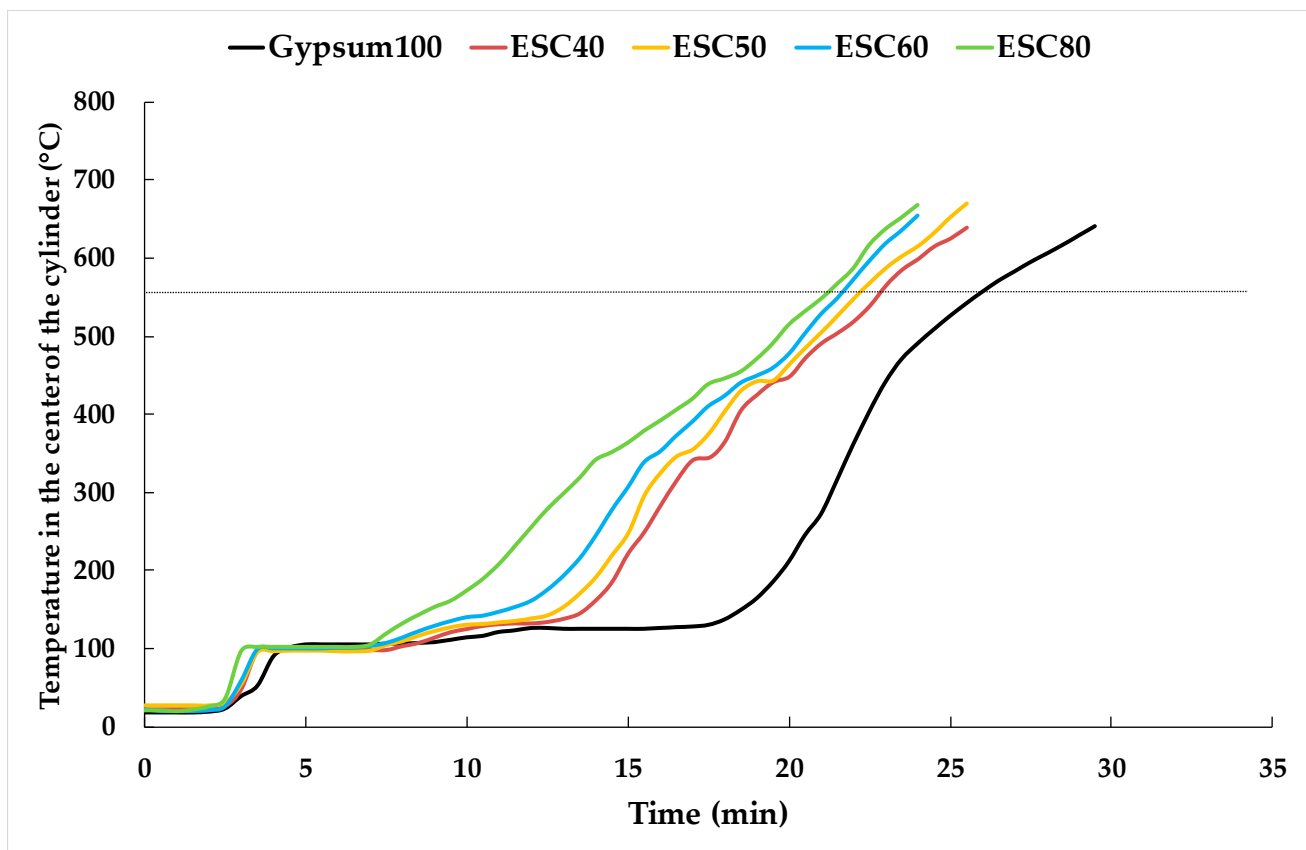


Figure 11. Fire insulating capacity of the different mixtures.

### 3.5. Leaching Results

The composition of leaching components, including contaminants, naturally depends on the amounts of the components present in the waste. Table 3 presents the results of the leaching tests conducted on the slag and commercial gypsum. Of the elements analyzed, Ba exhibits the highest leaching percentage (3.8% of its presence in the ladle slag). When compared to gypsum, ladle slag demonstrates a higher leaching capacity for Ba, as well as slightly elevated levels of Zn and Cu.

A European directive categorizes waste into three classifications: inert, non-hazardous, and hazardous. Table 3 juxtaposes the leaching data from ladle slag and commercial gypsum with the established limits outlined in the European directive [38]. Based on these results, ladle slag can be categorized as inert waste. Throughout their useful life, construction materials should not have a substantial negative influence on the environment. Furthermore, building materials must not endanger the health, hygiene, or safety of tenants or employees. Although there is no particular consistent rule controlling heavy metal leaching in waste-containing building materials within the European Union, many countries have developed their own regulations. For example, Portugal [39] has established a national regulation, while Spain has implemented regional regulations in areas such as the Basque Country [40], Catalonia [41], and Cantabria [42] for the recycling of waste in construction materials, following the European standard leaching test EN12457-4 [32]. These regulations employ the same test methodology but define distinct limits for certain elements. In Portugal, recycling of waste is permitted by the Portuguese Environment Agency as long as the limits for inert waste are not exceeded, thus making ladle slag eligible for recycling.

**Table 3.** Results of the EN 12457-4 (mg/kg, dry basis) alongside the prescribed limits delineated in the European landfill directive and Spanish regional regulations [40–42].

Element	Ladle Slag	Gypsum	Catalonia and Cantabria Limits	Basque Country Limit	Inert Waste	Non-Hazardous Waste
Zn	0.32	<0.25	4	1.2	4	50
V	<0.05	<0.05	-	1.3	-	-
Se	<0.25	<0.02	0.1	0.007	0.1	0.5
Pb	<0.1	<0.1	0.5	-	0.5	10
Ni	<0.05	<0.05	0.4	0.8	0.4	10
Mo	<0.1	<0.1	0.5	1.3	0.5	10
Hg	<0.01	<0.01	0.01	-	0.01	0.2
Sb	<0.1	<0.05	0.06	-	0.06	0.7
Cu	0.073	<0.05	2	-	2	50
Cr	<0.05	<0.05	0.5	2.6	0.5	10
Co	<0.05	<0.05	-	-	-	-
Cd	<0.02	<0.02	0.04	0.009	0.04	1
Ba	11.2	0.6	20	17	20	100
As	<0.25	<0.25	0.5	-	0.5	2

#### 4. Conclusions

Ladle slag has a great potential to be used as a component of alternative products to gypsum-based fire-resistant commercial materials. The developed product presents similar fire resistance, physical, and mechanical properties to other commercial products used in passive fire protection in buildings.

The following conclusions are made:

- In terms of physical characteristics, the substitution of gypsum with ladle slag leads to a reduction in density due to its higher specific gravity.
- In terms of mechanical standpoint, the incorporation of ladle slag has a diminishing effect on mechanical properties. Dosages equal to lower than 60%wt of ladle slag exhibit compressive strengths exceeding 2 MPa. The surface hardness exceeds the limit for high-density materials in compositions with a ladle slag content lower than 50%, which represents the only restriction concerning ladle slag recycling.
- The compressive strength decreases with increasing temperatures, but the reduction in compressive strength at elevated temperatures is proportionally lower when the slag content is higher.
- The fire insulating capacity of the mixtures diminishes as the proportion of slag increases, although the inclusion of ladle slag exhibits some positive influence on its fire insulating capacity due to certain endothermic processes (resulting in a 20% reduction when 60% weight of slag is used). Notably, no gas emissions were observed during the fire test.
- Ladle slag can be effectively used as a component in construction materials, in terms of heavy metals leaching.

According to these conclusions, fire insulating gypsum-based materials with a ladle slag content lower than 50%, could satisfy all the physical and mechanical requirements of gypsum-based materials, with a similar fire resistance.

**Author Contributions:** Conceptualization, C.L. and B.P.; methodology, C.L.; formal analysis, C.L. and B.P.; investigation, B.P. and E.M.P.-S.; data curation, E.M.P.-S. and Y.L.-G.; writing—original draft preparation, C.L.; writing—review and editing, E.M.P.-S.; project administration, Y.L.-G.; funding acquisition, Y.L.-G. All authors have read and agreed to the published version of the manuscript.

**Funding:** This research was funded by the Ministerio de Ciencia e Innovación of Spain under project number PID2019-110928RB-C33.

**Institutional Review Board Statement:** Not applicable.

**Informed Consent Statement:** Not applicable.

**Data Availability Statement:** Not applicable.

**Conflicts of Interest:** The authors declare no conflict of interest.

## References

1. Steel Statistical Yearbook 2020 Concise Version, World Steel Association. 2020. Available online: <https://worldsteel.org/wp-content/uploads/Steel-Statistical-Yearbook-2020-concise-version.pdf> (accessed on 19 September 2023).
2. Wu, L.; Li, H.; Mei, H.; Rao, L.; Wang, H.; Lv, N. Generation, utilization, and environmental impact of ladle furnace slag: A minor review. *Sci. Total Environ.* **2023**, *895*, 165070. [[CrossRef](#)] [[PubMed](#)]
3. Shi, C. Characteristics and cementitious properties of ladle slag fines from steel production. *Cem. Concr. Res.* **2002**, *32*, 459–462. [[CrossRef](#)]
4. Pachta, V.; Anastasiou, E.K. Utilization of industrial byproducts for enhancing the properties of cement mortars at elevated temperatures. *Sustainability* **2021**, *13*, 12104. [[CrossRef](#)]
5. Santamaría, A.; Ortega-López, V.; Skaf, M.; Faleschini, F.; Orbe, A.; San-José, J.T. 23—Ladle furnace slags for construction and civil works: A promising reality. In *Waste and Byproducts in Cement-Based Materials—Innovative Sustainable Materials for a Circular Economy*; de Brito, J., Thomas, C., Medina, C., Agrela, F., Eds.; Woodhead Publishing: Cambridge, UK, 2021; pp. 659–679. [[CrossRef](#)]
6. Pasetto, M.; Baliello, A.; Giacomello, G.; Pasquini, E. The use of steel slags in asphalt pavements: A state-of-the-art review. *Sustainability* **2023**, *15*, 8817. [[CrossRef](#)]
7. Skaf, M.; Ortega-Lopez, V.; Fuente-Alonso, J.A.; Santamaria, A.; Manso, J.M. Ladle furnace slag in asphalt mixes. *Constr. Build. Mater.* **2016**, *122*, 488–495. [[CrossRef](#)]
8. Shih, P.-H.; Chang, Y.-K.; Dai, H.-A.; Chiang, L.-C. Porous fire-resistant materials made from alkali-activated electric arc furnace ladle slag. *Processes* **2022**, *10*, 638. [[CrossRef](#)]
9. Gómez-Casero, M.Á.; Pérez-Villarejo, L.; Sánchez-Soto, P.J.; Eliche-Quesada, D. Alkali activated cements based on slags from different industries. *Mater. Proc.* **2022**, *8*, 123. [[CrossRef](#)]
10. Rodríguez, A.; Manso, J.M.; Aragón, Á.; González, J.J. Strength and workability of masonry mortars manufactured with ladle furnace slag. *Resour. Conserv. Recycl.* **2009**, *53*, 645–651. [[CrossRef](#)]
11. Montenegro, J.M.; Celemín-Matachana, M.; Cañizal, J.; Setién, J. Ladle furnace slag in the construction of embankments: Expansive behavior. *J. Mater. Civ. Eng.* **2013**, *25*, 972–979. [[CrossRef](#)]
12. Ghisman, V.; Muresan, A.C.; Buruiana, D.L.; Axente, E.R. Waste slag benefits for correction of soil acidity. *Sci. Rep.* **2022**, *12*, 16042. [[CrossRef](#)]
13. Setién, J.; Hernández, D.; González, J.J. Characterization of ladle furnace basic slag for use as a construction material. *Constr. Build. Mater.* **2009**, *23*, 1788–1794. [[CrossRef](#)]
14. Yew, M.C.; Yew, M.K.; Yuen, R.K.K. Experimental analysis of lightweight fire-rated board on fire resistance, mechanical, and acoustic properties. *Fire* **2023**, *6*, 221. [[CrossRef](#)]
15. Vilches, L.F.; Leiva, C.; Vale, J.; Fernández-Pereira, C. Insulating capacity of fly ash pastes used for passive protection against fire. *Cem. Concr. Compos.* **2005**, *27*, 776–781. [[CrossRef](#)]
16. Vilches, L.F.; Leiva, C.; Olivares, J.; Vale, J.; Fernández, C. Coal fly ash-containing sprayed mortar for passive fire protection of steel sections. *Mater. Constr.* **2005**, *55*, 25–37. [[CrossRef](#)]
17. García Arenas, C.; Marrero, M.; Leiva, C.; Solís-Guzmán, J.; Vilches Arenas, L.F. High fire resistance in blocks containing coal combustion fly ashes and bottom ash. *Waste Manag.* **2011**, *31*, 1783–1789. [[CrossRef](#)]
18. Peceño, B.; Pérez-Soriano, E.M.; Ríos, J.D.; Luna, Y.; Cifuentes, H.; Leiva, C. Effect of different ashes from biomass olive pomace on the mechanical and fire properties of gypsum-based materials. *Rev. Constr.* **2023**, *22*, 122–134. [[CrossRef](#)]
19. Leiva, C.; Vilches, L.F.; Vale, J.; Fernández-Pereira, C. Fire resistance of biomass ash panels used for internal partitions in buildings. *Fire Saf. J.* **2009**, *44*, 622–628. [[CrossRef](#)]
20. Gutiérrez-González, S.; Gadea, J.; Rodríguez, A.; Blanco-Varela, M.T.; Calderón, V. Compatibility between gypsum and polyamide powder waste to produce lightweight plaster with enhanced thermal properties. *Constr. Build. Mater.* **2012**, *34*, 179–185. [[CrossRef](#)]
21. Peceño, B.; Alonso-Fariñas, B.; Vilches, L.F.; Leiva, C. Study of seashell waste recycling in fireproofing material: Technical, environmental, and economic assessment. *Sci. Total Environ.* **2021**, *790*, 148102. [[CrossRef](#)]
22. Salazar, P.A.; Fernández, C.L.; Luna-Galiano, Y.; Sánchez, R.V.; Fernández-Pereira, C. Physical, mechanical and radiological characteristics of a fly ash geopolymer incorporating titanium dioxide waste as passive fire insulating material in steel structures. *Materials* **2022**, *15*, 8493. [[CrossRef](#)]
23. Ríos, J.D.; Arenas, C.; Cifuentes, H.; Vilches, L.F.; Leiva, C. Development of a paste for passive fire protection mainly composed of granulated blast furnace slag. *Environ. Prog. Sustain. Energy* **2020**, *39*, e13382. [[CrossRef](#)]
24. Gutiérrez-González, S.; Gadea, J.; Rodríguez, A.; Junco, C.; Calderón, V. Lightweight plaster materials with enhanced thermal properties made with polyurethane foam wastes. *Constr. Build. Mater.* **2012**, *28*, 653–658. [[CrossRef](#)]
25. Alonso, A.; Rodríguez, A.; Gadea, J.; Gutiérrez-González, S.; Calderón, V. Impact of plasterboard with ladle furnace slag on fire reaction and thermal behavior. *Fire Technol.* **2019**, *55*, 1733–1751. [[CrossRef](#)]

26. EN 13279-1:2009; Gypsum Binders and Gypsum Plasters—Part 1: Definitions and Requirements. European Committee for Standardization (CEN): Brussels, Belgium, 2009. [[CrossRef](#)]
27. UNE-EN 1097-3:1999; Tests for Mechanical and Physical Properties of Aggregates—Part 3: Determination of Loose Bulk Density and Voids. Spanish Association for Standardization and Certification (UNE): Madrid, Spain, 1999.
28. EN 12859:2012; Gypsum Blocks—Definitions, Requirements and Test Methods. Spanish Association for Standardization and Certification (UNE): Madrid, Spain, 2012.
29. ASTM E761/E761M-92(2020); Standard Test Method for Compressive Strength of Sprayed Fire-Resistive Material Applied to Structural Members. American Society for Testing and Materials: West Conshohocken, PA, USA, 2020.
30. EN 1363-1:2021; Fire Resistance Tests—Part 1: General Requirements. Spanish Association for Standardization and Certification (UNE): Madrid, Spain, 2021.
31. Serjun, V.Z.; Mladenovic, A.; Mirtič, B.; Meden, A.; Ščančar, J.; Milačič, R. Recycling of ladle slag in cement composites: Environmental impacts. *Waste Manag.* **2015**, *43*, 376–385. [[CrossRef](#)]
32. EN 12457-4:2003; Characterisation of Waste—Leaching—Compliance Test for Leaching of Granular Waste Materials and Sludges—Part 4: One Stage Batch Test at a Liquid to Solid Ratio of 10 L/kg for Materials with Particle Size Below 10 mm (without or with Size Reduction). Spanish Association for Standardization and Certification (UNE): Madrid, Spain, 2003.
33. Aponte, D.; Soto Martín, O.; Valls del Barrio, S.; Barra Bizinotto, M. Ladle steel slag in activated systems for construction use. *Minerals* **2020**, *10*, 687. [[CrossRef](#)]
34. EN 1097-7:2009; Tests for Mechanical and Physical Properties of Aggregates—Part 7: Determination of the Particle Density of Filler—Pyknometer Method. Spanish Association for Standardization and Certification (UNE): Madrid, Spain, 2009.
35. Luo, Y.; Klima, K.M.; Brouwers, H.J.H.; Yu, Y. Effects of ladle slag on Class F fly ash geopolymers: Reaction mechanism and high temperature behavior. *Cem. Concr. Compos.* **2022**, *129*, 104468. [[CrossRef](#)]
36. Adesanya, E.; Sreenivasan, H.; Kantola, A.M.; Telkki, V.-V.; Ohenoja, K.; Kinnunen, P.; Illikainen, M. Ladle slag cement—Characterization of hydration and conversion. *Constr. Build. Mater.* **2018**, *193*, 128–134. [[CrossRef](#)]
37. Leiva, C.; García Arenas, C.; Vilches, L.F.; Vale, J.; Gimenez, A.; Ballesteros, J.C.; Fernández-Pereira, C. Use of FGD gypsum in fire resistant panels. *Waste Manag.* **2010**, *30*, 1123–1129. [[CrossRef](#)] [[PubMed](#)]
38. Council Directive 1999/31/EC of 26 April 1999 on the Landfill of Waste. Official Journal L 182, 16/07/1999 P. 0001–0019. European Commission, 1999. Available online: <http://data.europa.eu/eli/dir/1999/31/oj> (accessed on 19 September 2023).
39. DL 183/2009 Waste Disposal at Landfills. Transposition to the Portuguese Law of Council. Directive 1999/31/CE, April 26. Portuguese Mint and Official Printing Office: Lisbon, Portugal, 2009.
40. Decreto 34 del País Vasco Por el Que Se Regula la Valorización y Posterior Utilización de Escorias Procedentes de la Fabricación de Acero en Hornos de arco Eléctrico, en el Ámbito de la Comunidad Autónoma del País Vasco. País Vasco, Spain. 2003. Available online: <https://www.legegunea.euskadi.eus/eli/es-pv/d/2003/02/18/34/dof/spa/html/webleg00-contfich/es/> (accessed on 19 September 2023).
41. Decreto 32/2009 de 24 de Febrero Sobre la Valorización de Escorias Siderúrgicas; Generalitat de Catalunya: Barcelona, Spain, 2009. Available online: [http://www.arc.cat/es/publicacions/pdf/normativa/catalana/decrets/decret\\_32\\_2009.pdf](http://www.arc.cat/es/publicacions/pdf/normativa/catalana/decrets/decret_32_2009.pdf) (accessed on 19 September 2023).
42. Decreto 100/2018 de Valorización de Escorias en la Comunidad Autónoma de Cantabria. Cantabria, Spain. 2019. Available online: <https://boc.cantabria.es/boces/verAnuncioAction.do?idAnuBlob=333876> (accessed on 19 September 2023).

**Disclaimer/Publisher’s Note:** The statements, opinions and data contained in all publications are solely those of the individual author(s) and contributor(s) and not of MDPI and/or the editor(s). MDPI and/or the editor(s) disclaim responsibility for any injury to people or property resulting from any ideas, methods, instructions or products referred to in the content.